

Increasing the Fisher Information Content in the Matter Power Spectrum through Reconstruction

Qiaoyin Pan,^{1,*} Ue-Li Pen,^{2,3,4,5,†} Derek Inman,^{6,7} and Hao-Ran Yu^{8,2}

¹*School of Physics, Nankai University, 94 Weijin Rd, Nankai, Tianjin, 300071, China*

²*Canadian Institute for Theoretical Astrophysics,
University of Toronto, M5S 3H8, Ontario, Canada*

³*Dunlap Institute for Astronomy and Astrophysics,
University of Toronto, Toronto, ON M5S 3H4, Canada*

⁴*Canadian Institute for Advanced Research, Program in Cosmology and Gravitation*

⁵*Perimeter Institute for Theoretical Physics, Waterloo, ON, N2L 2Y5, Canada*

⁶*Canadian Institute for Theoretical Astrophysics, University of Toronto,
60 St. George St., Toronto, ON M5S 3H8, Canada*

⁷*Department of Physics, University of Toronto, 60 St. George, Toronto, ON M5S 1A7, Canada*

⁸*Department of Astronomy, Beijing Normal University, Beijing, 100875, P.R.China*

(Dated: November 3, 2016)

We adapt a new reconstruction method called Adaptive particle mesh (APM) to 136 non-linear density fields given by independent N-body simulations, in order to recover some of the information lost in the non-linear regime of large-scale structure. Through analyzing the power spectra of both density fields from simulations and deformation potentials from reconstructions, we find that after reconstruction, the non-linear regime of correlation matrix sinks to some extent. We also find that the Fisher information has a increase by a factor up to 20 at the translinear plateau.

PACS numbers:

I. INTRODUCTION

Power spectrum of matter density field is essential in modern cosmology research since it is related to many cosmology parameters. Many dedicated experiments attempt to constrain some specific parameters. Fisher information is widely used for making predictions for the errors and covariances of parameter estimates. Rimes and Hamilton[1] first studied the Fisher information as a function of scale contained in the matter power spectrum given by N-body simulation, and find that there's a plateau at translinear scales ($k \simeq 0.2 - 0.8 h\text{Mpc}^{-1}$), which showed that in this region, power spectrum contains little information over and above that in the linear power spectrum. Apart from numerical trend, Fisher information was also estimated in data from observation. For example, Lee and Pen [2] measured the information content in the galaxy angular power spectrum with the help of the Rimes-hamilton technique, and also found that the information saturation. After that, many approaches were put forward to recover parts of the lost information in the power spectrum of matter density field, aiming at the information function closer to that of the power spectrum for linear density fields. Neyrinck, Szapudi and Rimes [3] argued that more information could be extracted on non-linear scales if the masses of the largest haloes in a survey are known. Neyrinck, Szapudi and Szalay [4] found that nonlinearities in the dark-matter power spectrum are dramatically smaller if the density field first undergoes a logarithmic mapping, yielding 10 times more cumulative signal-to-noise at $z = 0$.

Zhang et al. [5] suggested that using Wavelet Wiener filter to separate Gaussian and non-Gaussian structure in wavelet space is possible to increase the Fisher information by a factor of three before reaching the translinear plateau. Similar steps was also done in the angular power spectrum of weak lensing [6] and the result showed that there's three times more information compared to that of logarithmic mapping. Later, Neyrinck [7] applied Gaussianizing transformation method to cosmology and found that it can greatly multiply the Fisher information. Simpson, Heavens and Heymans utilized Clipping [8] technique on the matter density field and found it increased the number of useful Fourier modes by more than two orders of magnitude. Pen [9, 10] introduced new N-body algorithm call Adapted Particle-mesh (APM), which scaled linearly with the number of particles for the computational effort per time step, aiming at offering higher resolution. This method can be used to reconstruct the matter density field and is hopeful for tracing a non-linear density field back to its linear part[11]. This paper is organized as follows. In Section II, we present the main steps of the N-body simulation code that was used to simulate the dark matter density fields. In Section III, we briefly describe the reconstruction algorithm. In Section IV, we calculate and compare the power spectra, correlation matrix and Fisher information given by simulation and reconstruction. Conclusion and discussion are presented in Section V

II. N-BODY SIMULATION OF DARK MATTER DENSITY FIELDS

We run 136 simulations with a box size of $300 h^{-1}\text{Mpc}$, resolution of 1024^3 cells and 512^3 particles, using the cosmological simulation code CubeP3M(CITA Comput-

*Electronic address: panda@mail.nankai.edu.cn

†Electronic address: pen@cita.utoronto.ca

ing 2008). The initial condition is given by reading CMB-FAST transfer function and then evolving the power linearly to $z = 100$. Then Zel'dovich approximation is used to calculate the displacement field and velocity field, which are assigned to the particles. The cosmological parameters used are $\Omega_M = 0.32$, $\Omega_\Lambda = 0.679$, $h = 0.67$, $\sigma_8 = 0.83$, and $n_s = 0.96$. And we use different seeds to produce the initial conditions for different simulations so that those simulations are independent to each other. Then the initial densities are evolved up to $z = 0$. One layer of one of those $\log(\delta + 1)$ fields is plotted in Fig. II (a), in which the magnitude is the average of number of particles per cell over the dimension perpendicular to the paper.

III. RECONSTRUCTION ALGORITHM

We use the algorithm and numerical method called Adaptive Particle-mesh (APM), described in [9, 10]. to reconstruct the density field. The basic idea is to build a PM scheme on a curvilinear coordinate system, in which the number of the particles per grid cell is set approximately constant. Consider a numerical grid of curvilinear coordinates $\xi = (\xi_1, \xi_2, \xi_3)$. In order to determine the physical position of each grid point, one needs to specify the Euclidean coordinate $\mathbf{x}(\xi, t)$ as a function of grid position. In the Euclidean coordinate, the flat metric is Kronecker delta function δ_{ij} , while the curvilinear metric is given by

$$g_{\mu\nu} = \frac{\partial x^i}{\partial \xi^\mu} \frac{\partial x^j}{\partial \xi^\nu} \delta_{ij}. \quad (1)$$

We use the convention that Latin indices denote Cartesian coordinate, while Greek indices denote the curvilinear grid coordinate. In principle, there are many different methods to connect the Cartesian coordinate and curvilinear coordinate of each grid cell. In APM method, the connection is described by an irrotational deformation,

$$x^i = \xi^\mu \delta_\mu^i + \Delta x^i, \quad (2)$$

where

$$\Delta x^i = \frac{\partial \phi}{\partial \xi^\nu} \delta_\nu^i. \quad (3)$$

This choice of the deformation can minimize mesh distortion and twisting. ϕ is called the deformation potential, and Δx^i the lattice displacement. The deformation potential can be given in terms of the continuity equation in curvilinear coordinate,

$$\frac{\partial \sqrt{g} \rho}{\partial t} + \partial_\mu [\rho \sqrt{g} e_\mu^i (v^i - \Delta \dot{x}^i)] = 0 \quad (4)$$

where $\sqrt{g} \equiv (\partial x^i / \partial \xi^\alpha)$ is the volume element and $e_\mu^i = \partial \xi^\mu / \partial x^i$ is the triad. $\Delta \dot{x} = \delta^{i\nu} \partial_\nu \dot{\phi}$ is chosen such that the first term in equation 4 is zero, resulting in a constant mass per volume element. And the velocity field divergence is replaced by the deviation density field

$\Delta \rho = \bar{\rho} - \rho \sqrt{g}$, which ideally should be zero. Then the deformation potential is described in the elliptic equation,

$$\partial_\mu (\rho \sqrt{g} e_\mu^i \delta^{i\nu} \partial_\nu \Delta \phi) = \Delta \rho \quad (5)$$

The equation 5 can be solved using multigrid algorithm described in Ref. Then the displacement is given by the gradient of the deformation potential as in 3. One layer of the deformed grids and the original density field of that layer is given in Fig. II (b). As expected, there's no grid crossing after reconstruction.

IV. POWER SPECTRA AND INFORMATION CONTENT

The power spectrum is the Fourier transform of the correlation function and measures the amount of clustering in the matter distribution in terms of the wavenumber k in unit of $h\text{Mpc}^{-1}$,

$$\langle \delta(\mathbf{k}) \delta(\mathbf{k}') \rangle = (2\pi)^3 P(\mathbf{k}) \hat{\delta}(\mathbf{k} - \mathbf{k}'), \quad (6)$$

where $\delta(\mathbf{k})$ is the density fluctuation in wave space, while $\hat{\delta}$ is the delta function. Of equal interest is Δ_k^2 , the power spectrum in its dimensionless form, defined as

$$\Delta_k^2 \equiv \frac{k^3 P(k)}{2\pi^2} \quad (7)$$

The power spectra of the mass distributions are calculated using the "Nearest Grid Point" (NGP) mass assignment scheme, which calculates the position of each particle based on which grid point it is nearest. In Fig.... we plot the mean power spectrum (and error bars) of 139 density fields and reconstructed deformation potentials. To calculate the cumulative Fisher information of the density fields, the covariance matrix of the power spectra should be first given. Mathematically, the covariance matrix is defined as

$$\text{Cov}(k, k') \equiv \frac{1}{N-1} \sum_{i=1}^N [P_i(k) - \langle P(k) \rangle] [P_i(k') - \langle P(k') \rangle], \quad (8)$$

where angle brackets mean the expected values. The cross-correlation coefficient matrix, or for short, the correlation matrix, is a normalized version of the covariance matrix,

$$\text{Corr}(k, k') = \frac{\text{Cov}(k, k')}{\sqrt{\text{Cov}(k, k) \text{Cov}(k', k')}}. \quad (9)$$

The correlation matrices for density fields from simulations and deformation potentials from reconstructions are shown in Fig. 2. For the original density fields, the linear regime, where $k < 0.1$, is diagonal, while in the non-linear regime, the power spectra of different k modes are strongly correlated by at least 60%. For the reconstructed deformation potential correlation matrix,

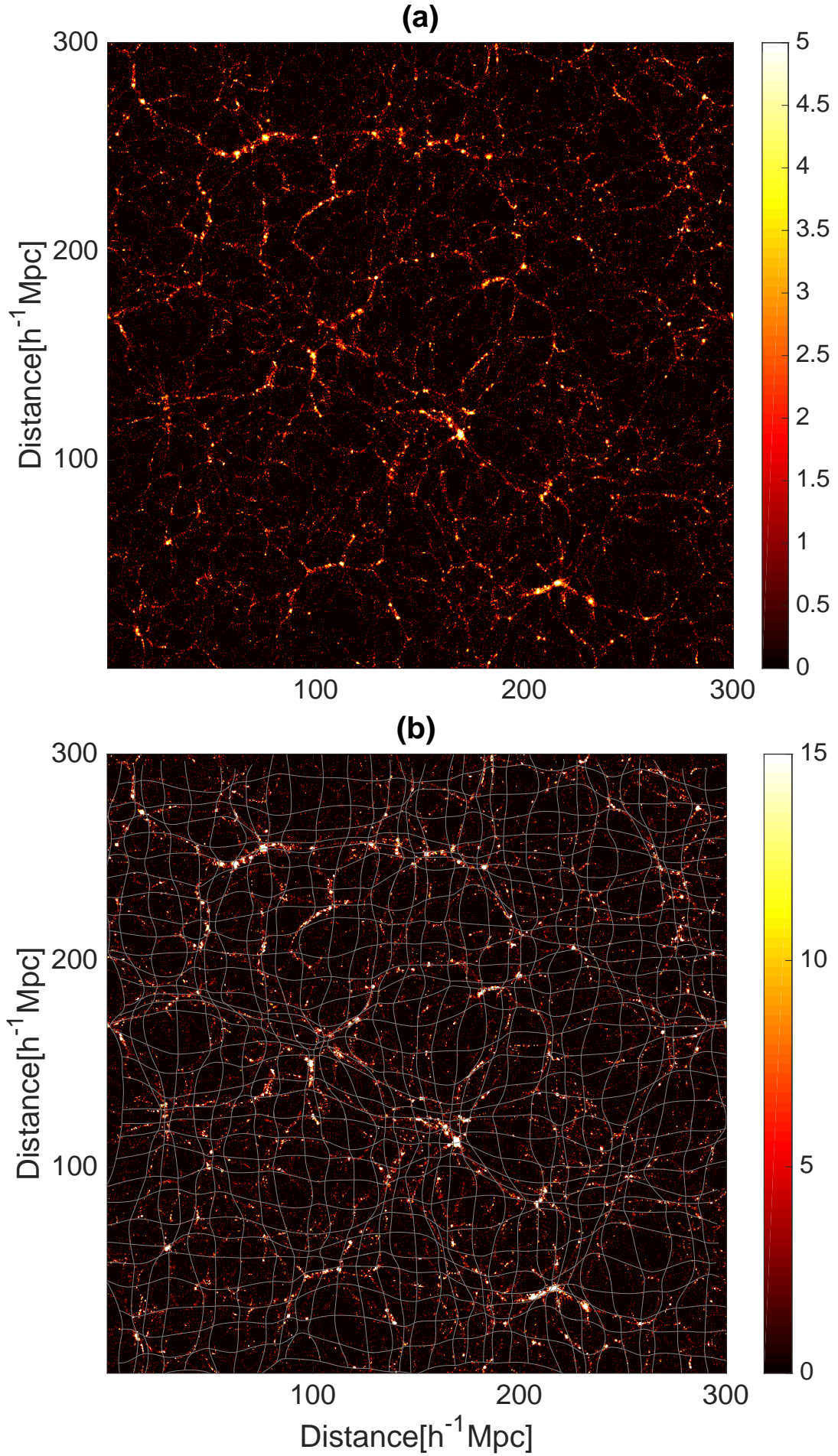


FIG. 1: (a) Map of a randomly selected $\log(\delta + 1)$ field from 136 N-body simulations, with a $300 h^{-1}$ Mpc width box and 1024^3 pixels. It's one layer of the whole box field, and the magnitude is the average of number of particles per cell. (b) The density field and the deformed grids of a random selected layer of the selected density field in (a)

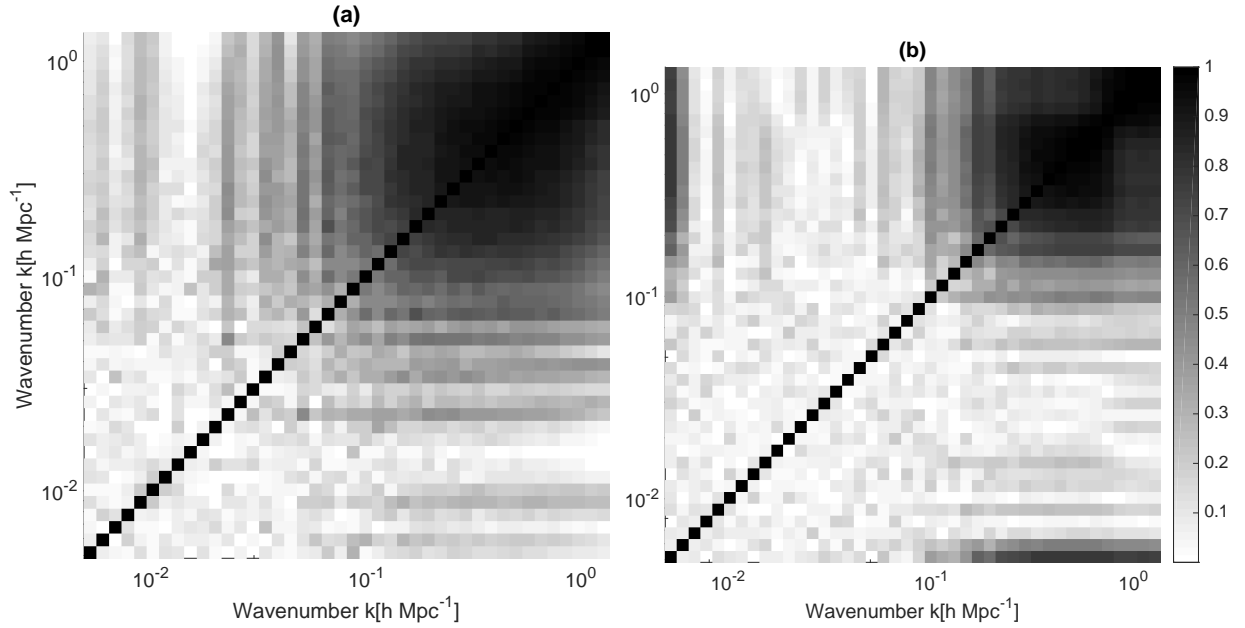


FIG. 2: Cross-correlation coefficient matrix as found from 136 power spectra of (a) the non-linear density field from simulation, (b) the deformation potential field from reconstruction

however, the linear regime expand up to k 0.2. The correlation matrix is closer to that for the power spectra of linear density fields. The cumulative, or Fisher, information function of k_n is then defined as the sum of the elements of inverse of subsection of the normalized covariance matrix up to k_n scale

$$I(< k_n) = \sum_{i,j=1}^n [C_{norm}^{-1}(k_i, k_j)] (i, j \leq n), \quad (10)$$

where C_{norm} is the normalized covariance matrix, defined as

$$C_{norm}(k, k') = \frac{\text{Cov}(k, k')}{\langle P(k) \rangle \langle P(k') \rangle}. \quad (11)$$

As seen above, cumulative information is a measurement of the number of independent Fourier modes presented in a field up to a given k_n , which represents how linear a field is. We plot the cumulative information of the power spectra of density fields from simulations and deformation potentials from reconstructions in Fig.3. In the translinear regime, where $k \sim 0.1$, the cumulative information of the non-linear density field has a flat plateau. It indicates that there's nearly no independent information in the translinear regime of the power spectrum. At $k \sim 0.8$, the information increase slightly again. But the information curve of the reconstructed deformation potential keeps increasing at that point and reaches it's plateau at $k \sim 0.4 - 0.5$ up to a factor of 20. It indicates that APM method can strongly recover the lost information within this scale.

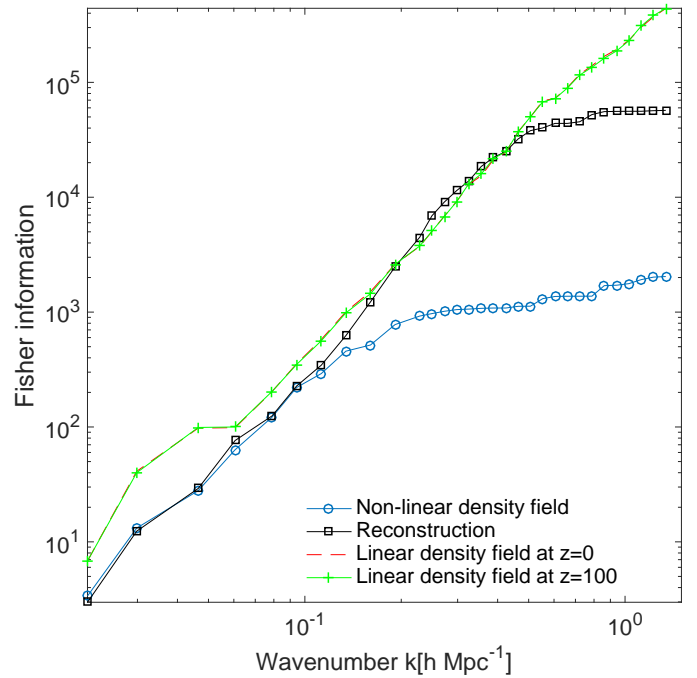


FIG. 3: Cumulative information in the power spectra as a function of wavenumber. The blue cycles correspond to the non-linear density field by simulation; the black squares correspond to the the reconstructed deformation potential; the red dash line corresponds to linear density field at $z=0$; the green crosses correspond to linear density field at $z=100$.

V. CONCLUSION AND DISCUSSION

We use the code "CubeP3M" to generate 137 independent dark matter density fields, then give the reconstructed deformation potentials which are pure divergent using APM method. We analyze the power spectra of both the density fields and the deformation potentials, after which we give the cross correlation matrix. We find that the power spectra are highly correlated on small scales, since these scales are in non-linear regime. But after reconstruction, the strongly correlated regime shinks from $k \sim 0.1$ to $k \sim 0.5$. We also calculate the cumulative information, and find that the plateau of the reconstructed information curve in the tranlinear regime rises by a factor of 20.

The new reconstruction method successfully recovers the lost linear information on the mildly non-linear scale, at least twice better than previous methods [3–7] and pushes the non-linear scale to a smaller scale in our case. The result in dark matter density fields gives a strong motivation to adapt APM method in halo fields, neutrino fields, etc, so that we have access to know more clearly about the physics in smaller scale. Some efforts were made to improve cosmology measurements to BAO scale

(e.g. [12, 13]). APM gives the reconstructed displacement given on the Lagrangian coordinate instead of the final Eulerian coordinate. It's successful try of BAO reconstruction in 1-D cosmology [11] provided an intuitive view of the algorithm to develop the BAO reconstruction in 3-D and thus push forward the BAO research.

APM method effectively decomposes the irrotational part and the curl part of the displacement field of particles, which would be meaningful to be compared with the decomposition of displacement field given by N-body simulation [14].

Acknowledgments

We thank Homg-Ming Zhu and Xin Wnag for friendly and helpful discussion. Computations were performed on the General Purpose Cluster supercomputer at the SciNet HPC Consortium. SciNet is funded by: the Canadian Foundation for Innovation under the auspices of Compute Canada; the Government of Ontario; Ontario Research Fund - Research Excellence; and the University of Toronto.

-
- [1] C. D. Rimes and A. J. S. Hamilton, in *American Astronomical Society Meeting Abstracts #207* (2006), vol. 207 of *American Astronomical Society Meeting Abstracts*, p. 206.01.
 - [2] J. Lee and U.-L. Pen, *ApJ* **686**, L1 (2008), 0807.1538.
 - [3] M. C. Neyrinck, I. Szapudi, and C. D. Rimes, *MNRAS* **370**, L66 (2006), astro-ph/0604282.
 - [4] M. C. Neyrinck, I. Szapudi, and A. S. Szalay, *ApJ* **698**, L90 (2009), 0903.4693.
 - [5] T.-J. Zhang, H.-R. Yu, J. Harnois-Déraps, I. MacDonald, and U.-L. Pen, *ApJ* **728**, 35 (2011), 1008.3506.
 - [6] H.-R. Yu, J. Harnois-Déraps, T.-J. Zhang, and U.-L. Pen, *MNRAS* **421**, 832 (2012), 1012.0444.
 - [7] M. C. Neyrinck, in *Statistical Challenges in 21st Century Cosmology*, edited by A. Heavens, J.-L. Starck, and A. Krone-Martins (2014), vol. 306 of *IAU Symposium*, pp. 251–254, 1407.4815.
 - [8] F. Simpson, A. F. Heavens, and C. Heymans, *Phys. Rev. D* **88**, 083510 (2013), 1306.6349.
 - [9] U.-L. Pen, *ApJS* **100**, 269 (1995).
 - [10] U.-L. Pen, *ApJS* **115**, 19 (1998), astro-ph/9704258.
 - [11] H.-M. Zhu, U.-L. Pen, and X. Chen, *ArXiv e-prints* (2016), 1609.07041.
 - [12] D. J. Eisenstein, H.-J. Seo, E. Sirko, and D. N. Spergel, *ApJ* **664**, 675 (2007), astro-ph/0604362.
 - [13] M. White, *MNRAS* **450**, 3822 (2015), 1504.03677.
 - [14] H.-R. Yu, U.-L. Pen, and H.-M. Zhu, *ArXiv e-prints* (2016), 1610.07112.
-